RET Inhibitor SPP86 Triggers Apoptosis and Activates the DNA Damage Response Through the Suppression of Autophagy and the PI3K/AKT Signaling Pathway in Melanoma Cells

Yuli Zhang [1,2], Haidong Liu[1], Kun Wang[3], Juan Zheng [4], Hong Luan[1], Ming Xin [5]

[1]Department of Dermatology, Liaocheng People's Hospital, Liaocheng, Shandong, People's Republic of China; [2]Department of Endocrinology, The Second Hospital of Shandong University, Jinan, Shandong, People's Republic of China; [3]Department of Endocrinology and Metabology, Liaocheng People's Hospital, Liaocheng, Liaocheng, Shandong, People's Republic of China; [4]Joint Laboratory for Translational Medicine Research, Liaocheng People's Hospital, Liaocheng, Shandong, People's Republic of China; [5]The Key Laboratory of Molecular Pharmacology, Liaocheng People's Hospital, Liaocheng, Shandong, People's Republic of China

Correspondence: Ming Xin, The Key Laboratory of Molecular Pharmacology, Liaocheng People's Hospital, Liaocheng, Shandong, People's Republic of China, Email xinming137@163.com; Hong Luan, Department of Dermatology, Liaocheng People's Hospital, Liaocheng, Shandong, People's Republic of China, Email lcsrmyy@126.com

Background: Melanoma is a highly lethal form of skin cancer, and effective treatment remains a significant challenge. SPP86 is a novel potential therapeutic drug. Nonetheless, the specific influence of SPP86 on autophagy, particularly its mechanisms in the context of DNA damage and apoptosis in human melanoma cells, remains inadequately understood. Thus, this study aims to explore the effects of SPP86 on autophagy and to elucidate its association with cell proliferation, apoptosis, and DNA damage in melanoma cells.

Methods: This study assessed the anti-tumor effects of SPP86 on cell viability, colony formation, apoptosis, and DNA damage in two melanoma cell lines, A375 and A2058. Concurrently, the underlying mechanisms, including the PI3K/AKT signaling pathway and autophagy modulation, were also elucidated.

Results: The study demonstrated that SPP86 exerts anti-tumor effects in melanoma cells through multiple mechanisms: it induces apoptosis, causes DNA damage, inhibits cell proliferation, and suppresses the PI3K/AKT signaling pathway. Importantly, the inhibition of autophagy appears to be a critical component of SPP86's mode of action, with the modulation of autophagic processes influencing the cytotoxicity against melanoma cells.

Conclusion: These promising findings suggest that SPP86 is a potential drug candidate for the treatment of melanoma, warranting further research and development.

Keywords: melanoma, SPP86, autophagy, DNA damage, apoptosis, PI3k/AKT

Introduction

Malignant melanoma (MM) is a highly invasive and metastatic cancer originating from melanocytes, which are most commonly found in the skin, but can also occur on mucosal surfaces and within visceral structures. Cutaneous melanoma (CM) accounts for a significant proportion of skin cancer mortality, causing 65% of deaths despite representing only 3% of skin cancer cases.[1] The incidence of CM has been increasing at an alarming rate worldwide, outpacing other cancers in terms of growth.[2,3] While early detection and timely intervention can result in a cure rate exceeding 90%,[4] advanced stages of CM, particularly thick melanomas, are associated with high mortality rates.[5] Conventional treatments such as radiotherapy and chemotherapy are often the default for advanced melanoma; however, these approaches can be limited in effectiveness, carry significant side effects, and may lead to the development of drug resistance.[1] Consequently, there is an urgent need to identify and develop more effective pharmacological treatments for melanoma.

67

Tyrosine kinase inhibitors and immune checkpoint inhibitors have significantly improved patient outcomes in melanoma treatment.[6] The PI3K/AKT pathway, often found to be activated in melanoma, is influenced by receptor tyrosine kinase (RTKs), which are pivotal in initiating signaling cascades.[7,8] The Rearranged during Transfection (RET) gene encodes a receptor tyrosine kinase integral to cellular processes such as growth, viability, motility, and differentiation.[9] Approximately 40–50% of melanoma patients carry BRAF-activating mutations (mainly BRAF V600E).[10] The BRAF gene is involved in the mitogen-activated protein kinase (MAPK) pathway,[11] the reactivation of which is frequently observed in BRAF-mutant melanomas. Inhibition of AKT is sufficient to block the proliferation of BRAF v600 mutant melanoma cells, and this effect is stronger in combination with MEK inhibitors.[12] SPP86 is a targeted RET inhibitor that selectively disrupts the PI3K/AKT and MAPK pathways, which are stimulated by RET in MCF7 cells.[13] Synthesized by MCE (Cat No.: 1,357,349–91-7), SPP86 has shown promise in preclinical models, inhibiting tumor growth effectively in laboratory and in vivo studies.[9,13] However, research documenting the clinical efficacy of SPP86 in melanoma patients remains scarce, indicating a critical area for future investigation.

Autophagy is intricately linked with a multitude of human diseases, including various cancers. It is regulated by the PI3K/AKT signaling pathway, which is crucial in the development and progression of a broad spectrum of pathological conditions, notably malignancies.[14] Preclinical studies suggest that autophagy may initially suppress tumor growth; however, it appears to switch roles to support tumor cell survival once a tumor is established.[15] Consequently, understanding autophagy's role in melanoma could be pivotal for devising new therapeutic strategies. Inhibition of autophagy has emerged as a promising method to improve treatment outcomes for advanced melanoma.[16] Xian showed that Berbamine Hydrochloride effectively inhibits late autophagy by targeting lysosomal acidification.[17] A Phase I/II clinical trial by Mehnert et al using HCQ in combination with a MAPK inhibitor for the treatment of advanced BRAFV600 mutant melanoma demonstrated the potential of targeting autophagy in combination with targeted therapy for advanced melanoma.[18] Nonetheless, the specific influence of SPP86 on autophagy, particularly its mechanisms in the context of DNA damage and apoptosis in human melanoma cells, remains inadequately understood. Thus, this study aims to explore the effects of SPP86 on autophagy and to elucidate its association with cell proliferation, apoptosis, and DNA damage in melanoma cells.

Materials and Methods
Reagents
SPP86 (HY-110193) and bafilomycin A1/Baf A1 (HY-100558) were purchased from MCE (USA), while Rapamycin (MB1197) was procured from Meilunbio (China). Dimethyl sulfoxide (DMSO) served to dissolve and dilute all compounds within the culture medium. The following antibodies were used, Bcl-2 (12,789-1-AP, 1:1000), Bax (50599-2-Ig, 1:2000), PARP1 (13,371-1-AP, 1:500), Caspase 3 (19,677-1-AP, 1:1000), LC3 (14,600-1-AP, 1:1000), SQSTM1 (66,184-1-Ig, 1:1000), AKT (10176-2-AP, 1:1000), phospho-AKT (ser473, 66,444-1-Ig, 1:1000), α-Tubulin (66031-1-Ig, 1:1000) were purchased from Proteintech (China). PI3K (T40115, 1:1000), phospho-PI3K (Tyr467/199, T40116, 1:1000) were purchased from Abmart (China). GAPDH (5174s, 1:2000), β-actin (3700s, 1:2000), γ-H2AX (Ser139, 9718s, 1:1000) were purchased from Cell Signaling Technology (USA). Horseradish peroxidase (HRP)-conjugated secondary antibodies (ab205718, Rb: 1:20000, ab205719, Ms: 1:10,000), Goat anti-rabbit IgG H&L (Alexa Fluor® 594, ab150116, 1:500) and Goat anti-mouse IgG H&L (Alexa Fluor® 488, ab150077, 1:500) were procured from Abcam (UK).

Cell Culture
A375 (CL-0014) and A2058 (CL-0652) were kindly provided Procell Life Science & Technology Co., Ltd. These cell lines were cultured in DMEM medium (Gibco, 11995065) supplemented with 10% FBS (Abwbio, AB-FBS0500) and 1% penicillin-streptomycin. The cells were maintained in a humidified atmosphere with 5% CO_2 at 37°C. The medium was refreshed every 48 to 72 h.

CCK-8 Analysis

The effect of SPP86 on melanoma cell viability was assessed using the CCK-8 assay (Beyotime, C0039). The Cell Viability Kit (CCK-8) is utilized for analyzing cell proliferation and toxicity. Its fundamental principle relies on the reagent containing WST-8, which is reduced to a highly water-soluble yellow formazan dye by cellular dehydrogenases in the presence of the electron carrier 1-Methoxy PMS. The intensity of the color is proportional to cell proliferation and inversely proportional to cytotoxicity. 96-well plates were utilized for seeding 5×10^3 cells, which were subsequently incubated overnight. Subsequently, the culture medium was removed, and the cells were treated with varying concentrations (0.01, 0.1, 1, 10, 100 µM) of SPP86. Negative control wells received 0.1% DMSO. Following exposure for 24 or 48 h, 10 µL of CCK-8 solution was added to each well and incubated for an additional hour. Absorbance at 450 nm was determined using a microplate reader, and the IC_{50} value calculated.

Colony Formation

The effect of SPP86 on melanoma cell proliferation was evaluated using crystal violet staining. Cells were plated in a 6-well culture plate at a density of 600 cells per well. Once adhered, different concentrations of SPP86 (0, 1, 5, 10 µM) were added to each well and incubated for 24 h. We continuously cultured the cells for 14 days, changing the medium every 3 days while monitoring their status. Once cloning was complete, the cells were washed once with PBS and fixed for 30 minutes by adding 1 mL of 4% paraformaldehyde to each well. After another wash with PBS, the cells were stained for 20 minutes with 1 mL of crystal violet staining solution. The wells were then washed three times with PBS, air-dried, and photographed. Five independent experiments were conducted. Resulting colonies were then imaged and counted.

Hoechst 33342/PI Analysis

To quantitatively assess whether SPP86 induces cell death in melanoma cells, the Hoechst 33342/PI double staining assay (Beyotime, P0137) was employed for measurement. Cells were plated into 24-well plates at a density of 100,000 cells in 500 µL of cell suspension per well and treated with SPP86 at a concentration of 10 µM for 24 h. Each sample was transferred to a centrifuge tube and the supernatant subsequently spun down. Hoechst 33342 (which stains nuclei blue) and PI (which stains nuclei red) were then applied, and the cells incubated at 4°C for 20–30 minutes. Cells were subsequently washed with PBS. Cell membranes were stained with Dio (Beyotime, C1038) fluorescent dye. Co-localization of Hoechst 33342 (blue) and PI (red) signified cell death. Cell death was assessed by fluorescence microscopy.

TUNEL Analysis

The potential of SPP86 to induce apoptosis in melanoma cells was evaluated using a one-step TUNEL Apoptosis Detection Kit (Beyotime, C1088). Initially, cells were plated into 24-well plates at a density of 100,000 cells per well and treated with SPP86 at a concentration of 10 µM for 24 h. Following treatment, the cells were fixed with paraformaldehyde and permeabilized using 0.1% Triton X-100 (Beyotime, P0096). Subsequently, they were incubated with 50 µL of TUNEL reagent, which labels DNA breaks with a green fluorescent marker, at 37°C for 60 minutes. The cell nuclei were then counterstained with DAPI (Beyotime, P0131), imparting a blue fluorescence, for 15 minutes. Fluorescence microscopy was utilized to visualize the stained cells, and the rate of apoptosis was quantified based on the TUNEL-positive cells.

Immunofluorescence Analysis

Cells were inoculated onto cell crawls in 24-well plates and treated with 10 µM SPP86 for 24 h. Subsequently, the cells were washed with PBS and fixed with 4% paraformaldehyde (PFA) solution for 15 minutes. After another PBS wash, cell permeabilization was achieved by treating them with 0.1% Triton X-100 (Beyotime, P0096) in PBS for 5 minutes. The cells were then confined with 3% BSA in PBS for 30 minutes to prevent non-specific binding. Following the blocking step, the cells were incubated with the primary antibody (β-actin (3700s, 1:100), γ-H2AX (Ser139, 9718s, 1:100), LC3 (14,600-1-AP, 1:100), SQSTM1 (66,184-1-lg, 1:100), α-Tubulin(66031-1-Ig, 1:100)) at 4°C overnight. After washing off the excess primary antibody with PBS, the cells were incubated with a fluorescently-labeled secondary antibody at room

temperature for 1 h. Lastly, the nuclei were stained with an antifluorescence quenching solution that contains DAPI for 15 minutes. Fluorescence microscopy was utilized to observe and analyze the co-localization of fluorescent signals within each cell.

Western Blot Analysis

The medium in the 6-well plate was discarded, and the cells were rinsed with PBS. Cells were collected in Eppendorf tubes using a cell scraper, and proteins were extracted by lysing the cells on ice for 30 minutes with RIPA buffer (Beyotime, P0013) supplemented with protease and phosphatase inhibitors. Protein concentration was quantified using a BCA kit (Beyotime, P0010). 50 µL of 5× protein sampling buffer was added to the samples, which were then boiled for 10 minutes to denature the proteins. Proteins were separated by 10% SDS-PAGE (electrophoresis: 80 V for 30 minutes, then 120 V for 40 minutes) using 30 µg of protein samples, and the separated proteins were subsequently transferred to a PVDF membrane (100 V for 1h 30 minutes). The membrane was blocked with 5% skim milk powder (BD Difco™ Skim Milk, 232100) for one hour. It was then incubated overnight at 4°C with target primary antibodies: Bcl-2 (12,789-1-AP, 1:1000), Bax (50599-2-lg, 1:2000), PARP1 (13,371-1-AP, 1:500), Caspase 3 (19,677-1-AP, 1:1000), γ-H2AX (Ser139, 9718S, 1:1000), phospho-PI3K (Tyr467/199, T40116, 1:1000), GAPDH (5174S, 1:2000), β-actin (3700S, 1:2000), and α-Tubulin (66031-1-Ig, 1:1000). After primary antibody incubation, the membrane was rinsed three times with TBST and then incubated at room temperature for one hour with HRP((ab205718, 1:20,000) and mouse anti-Ms (ab205719, 1:10,000))-conjugated secondary antibodies(Goat anti-rabbit IgG H&L (Alexa Fluor® 594) (ab150116, 1:500), Goat anti-mouse IgG H&L (ab150116, 1:500)). The membrane was washed three times with TBST. Finally, the blots were developed and analyzed using an ECL chemiluminescence detection system. The relative expression level of the target protein was expressed as the ratio of the target protein to the internal reference protein.

Flow Cytometric Analysis

Apoptosis was detected using the FITC Annexin V Apoptosis Detection Kit (BD Pharmingen™, 556547). Adherent cells were digested with 0.25% trypsin (without EDTA), and the suspended cells were collected by centrifugation for 5–10 minutes at room temperature. After washing the cells with pre-cooled PBS, 300 µL of 1× Binding Buffer was added to resuspend the cells. Subsequently, 5 µL of Annexin V-FITC and 5 µL of PI were added, and the mixture was gently mixed and incubated at room temperature for 15 minutes, protected from light. Prior to analysis, 200 µL of 1× Binding Buffer was added. Flow cytometric analysis was performed using a CytoFLEX SRT flow cytometer (BECKMAN COULTER, BF17071).

Statistical Analysis

Each experiment was conducted a minimum of five times, and results are presented as the mean ± standard deviation (SD). For the assessment of statistical significance between two groups, a paired, two-tailed Student's t-test was employed. Comparisons among multiple groups were performed using one-way ANOVA, with GraphPad Prism 9.0 software (Dunnett's Test) utilized for post hoc multiple comparisons when necessary. Statistical significance was established at a p-value of less than 0.05.

Results

SPP86 has Been Shown to Reduce Cell Viability and Inhibit the Proliferation of Melanoma Cells

To evaluate the effects of SPP86 on cell proliferation, melanoma A375 and A2058 cell lines were exposed to various concentrations of SPP86 (0.01, 0.1, 1, 10, 100 µM). Following 24 and 48 h of treatment with SPP86, a decrease in cell viability was observed in both cell lines. The half-maximal inhibitory concentration (IC_{50}) values were calculated to be 12.18 ± 2.69 µM for A375 cells at 24 h and 8.05 ± 2.62 µM at 48 h, while A2058 cells had IC50 values of 17.78 ± 1.75 µM at 24 h and 12.58 ± 1.84 µM at 48 h (Figure 1). These findings suggest that SPP86 can effectively suppress the growth of both A375 and A2058 melanoma cells in a dose- and time-dependent manner. To evaluate the effects of SPP86 on cytotoxicity of
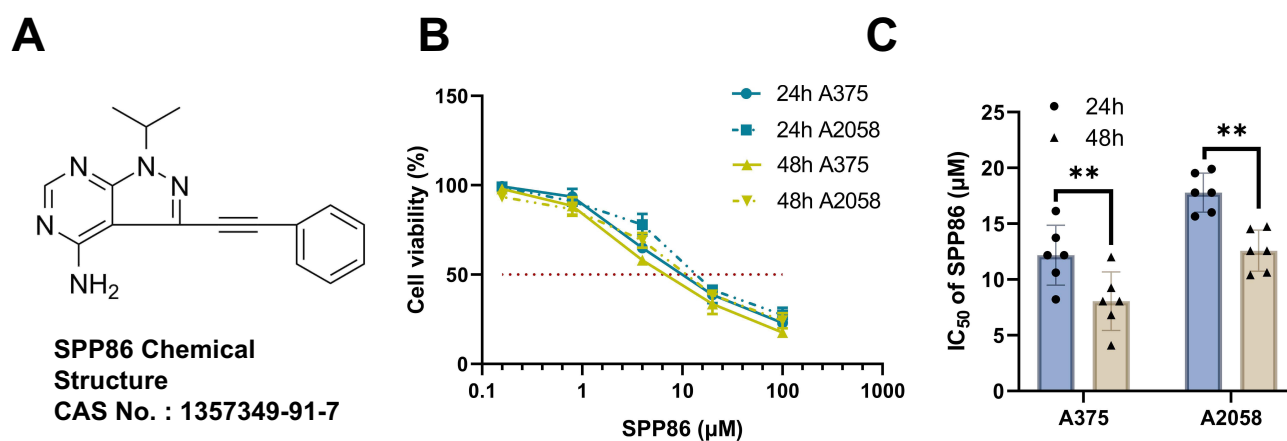
Figure I SPP86 reduced the viability of melanoma cells. (**A**) The chemical structure of SPP86. (**B**) A375 and A2058 cells were treated with increasing concentrations of SPP86 for 24 h and 48 h, the viability of A375 and A2058 cells were determined by CCK-8 assay. (**C**) The IC$_{50}$ values of SPP86 on A375 and A2058 cells. The data represent the mean ± SD from six independent experiments. **$P < 0.01$.

human normal HaCaT cells, HaCaT cells were exposed to various concentrations of SPP86 (0.01, 0.1, 1, 10, 100 μM). We found the IC$_{50}$ values to be 27.3 ± 1.98 μM (24 h) and 24.06 ± 2.70 μM (48 h). These results indicate that 10 μM of SPP86, when applied for 24 h, has a lesser effect on normal cells compared to cancer cells (Figure S1). Therefore, for the subsequent part of the experiment, we selected a concentration of 10 μM and an incubation period of 24 h for analysis.

## SPP86 Suppresses the Clone-Forming Ability of Melanoma Cells

Moreover, the suppressive effect of SPP86 on the clonogenic potential of A375 and A2058 cells was evaluated using a cell colony formation assay. The results revealed a reduction in the number of cell colonies at increasing concentrations of SPP86 (0, 1, 5, 10 μM) exposure (Figure 2). These findings provide convincing evidence that SPP86 suppresses the growth of human melanoma cells in a dose-dependent manner.

SPP86 Induces Apoptosis in Melanoma Cells

To determine if SPP86 could induce cell death, it was assessed using the Hoechst 33342/PI double staining kit. After 24 h of treatment with SPP86 (10 μM), it was observed that SPP86 significantly induced cell death in A375 and A2058 cells. The number of dead cells (red fluorescence) in cells treated with SPP86 was significantly higher than that in the corresponding controls, and apoptotic vesicles were also noted (Figure 3A and B).

To further ascertain if the cell death induced by SPP86 corresponded to apoptosis, the TUNEL apoptosis assay was conducted. Following 24 h of SPP86 (10 μM) treatment, the number of apoptotic cells (green fluorescence) in both cell lines was significantly higher than that in the corresponding control group, with a significant increase in the apoptosis rate observed (Figure 3C and D). Then we examined the effect of SPP86 on apoptosis of melanoma cells by Flow cytometry using Annexin V-FITC/PI Apoptosis Detection Kit. As shown in Figure S2, the percentage of apoptotic cells increased in a dose-dependent manner following treatment of A375 and A2058 cells with SPP86 (0, 5, and 10 μM). These results clearly indicate that SPP86 can induce cell death by promoting apoptosis (Figure S2).

To investigate the effect of SPP86 on apoptosis, the expression levels of apoptosis-related proteins were analyzed in A375 and A2058 cells treated with different concentrations of SPP86 for 24 h through Western blot analysis. The results indicated a dose-dependent increase in the Bax/Bcl-2 ratio relative to the control, implying the involvement of a mitochondrial pathway in apoptosis. To elucidate these mechanisms further, the expression of caspase-3 and its substrates PARP1 and their cleavage products were assessed. Levels of cleaved caspase-3 and cleaved PARP1 demonstrated a dose-dependent increase in cells treated with SPP86 relative to control cells. This result confirmed SPP86's pro-apoptotic effect at the molecular level (Figure 3E and F).

A

B
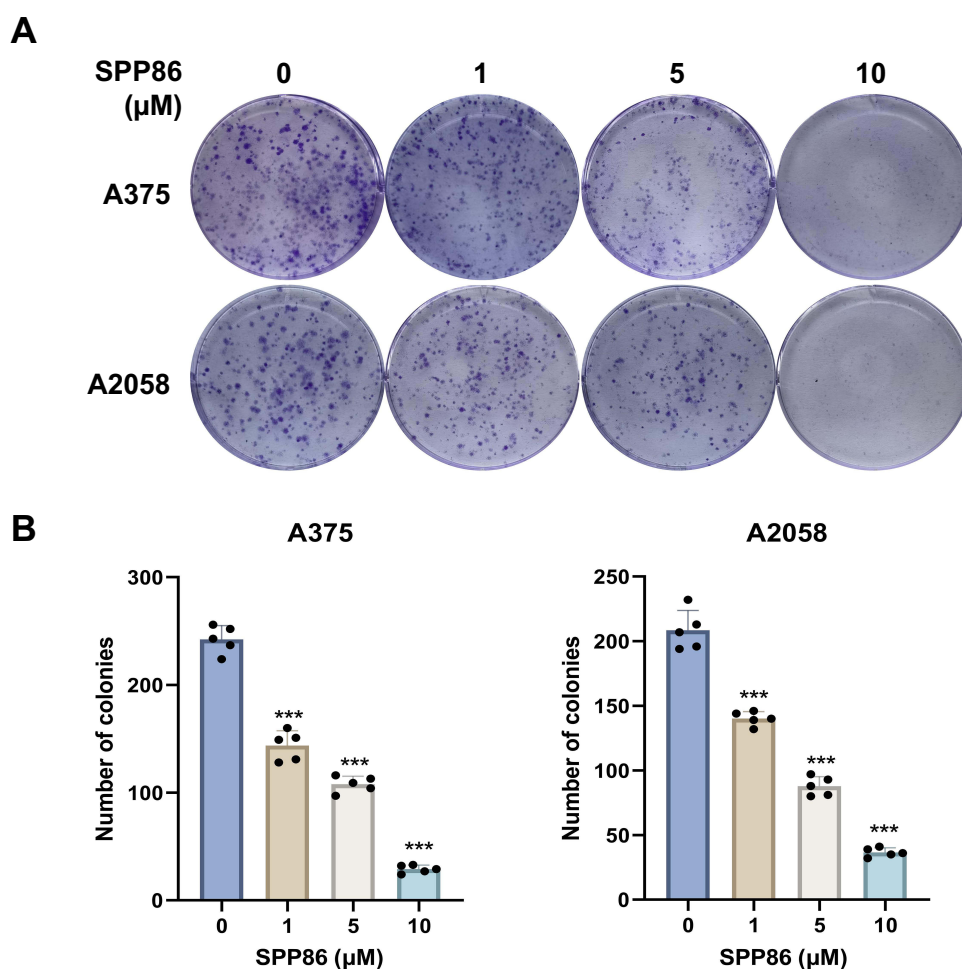
Figure 2 SPP86 inhibited cell colony formation of melanoma cells. (**A**) A375 and A2058 cells were treated with increasing concentrations of SPP86(0, 1, 5, 10 μM), the cell colonies were stained by crystal violet. (**B**) Statistically analyzed for clone formation. The data represent the mean ± SD from five independent experiments. $***P < 0.001$.

SPP86 Induces DNA Damage in Melanoma Cells

To study whether the cytotoxic effects of SPP86 are correlated with DNA damage, we evaluated its effect on the occurrence of DNA double-strand breaks (DSBs) by observing the development of γ-H2AX foci. The findings indicated that treatment with SPP86 for 24 h led to the presence of γ-H2AX foci in both A375 and A2058 cells (Figure 4A). Moreover, we confirmed the DNA damaging effects of SPP86 at the molecular level. Western blot were performed to determine the protein expression of γ-H2AX in A375 and A2058 cells treated with SPP86 for 24 h. Our results demonstrated that SPP86 upregulated the levels of γ-H2AX protein in both A375 and A2058 cells (Figure 4B).

SPP86 Inhibits Autophagy in Melanoma Cells

To evaluate the effect of SPP86 on autophagy in melanoma cells, by Immunofluorescence analysis, it was found that SPP86 treatment of cells promoted the formation of both LC3-labelled spots (green fluorescence) and SQSTM1-labelled spots (red fluorescence), indicating that autophagy was blocked (Figure 5A). The conversion ratio of LC3-II to LC3-I is considered a reliable indicator of autophagic activity. SQSTM1, a ubiquitin-binding protein that binds to LC3, was used to assess autophagic cargo recruitment and degradation. To explore the regulatory function of SPP86 in autophagy, we also assessed the conversion of endogenous LC3-I to LC3-II and SQSTM1 expression using immunoblotting. The results revealed that the LC3 II/I ratio and SQSTM1 expression were significantly increased in a dose-dependent manner after SPP86 treatment, indicating that autophagy was blocked, which further suggests that SPP86 inhibited cellular autophagy (Figure 5B).
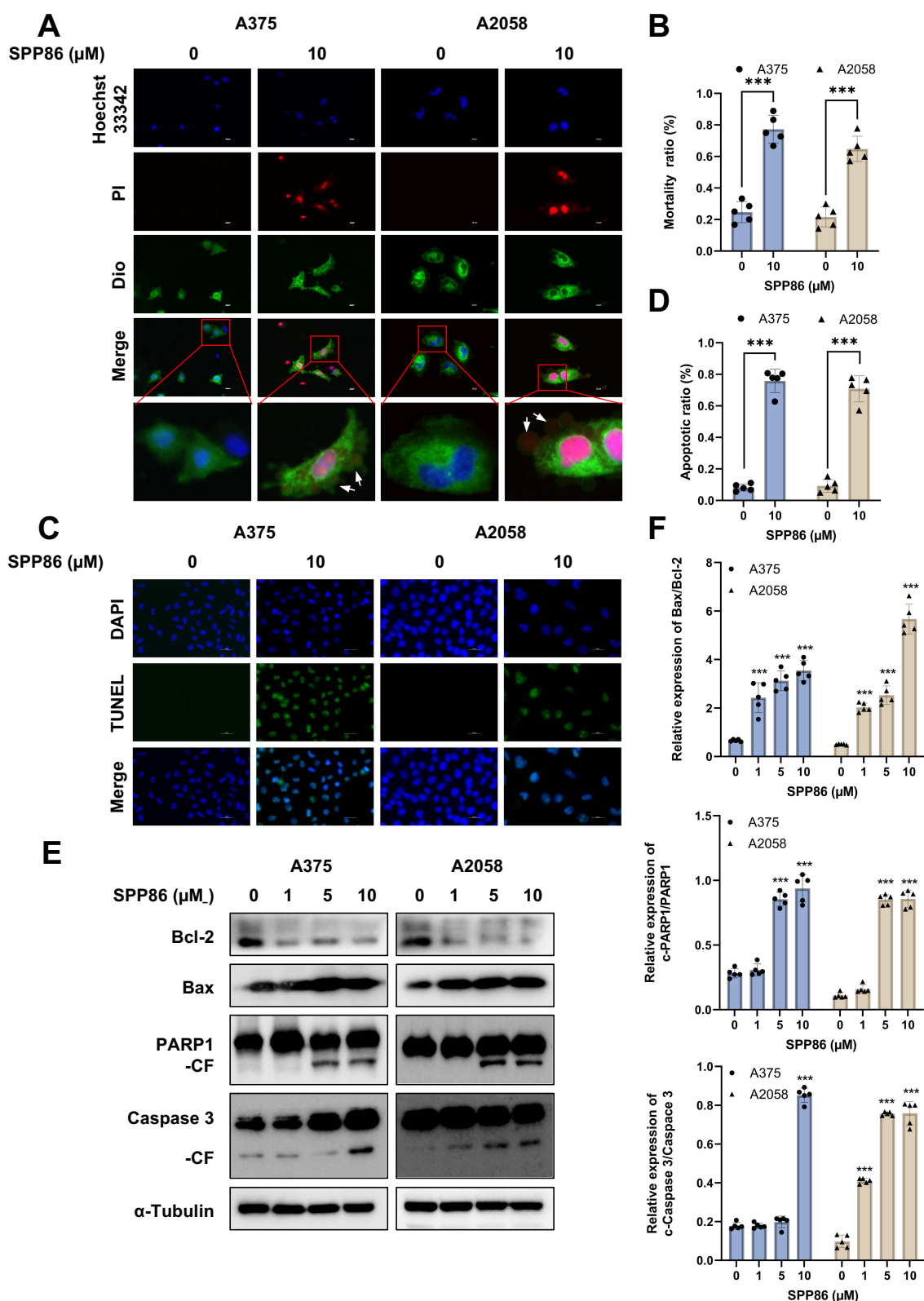
Figure 3 SPP86 induces apoptosis in melanoma cells. (**A** and **B**) A375 and A2058 cells were treated with SPP86 (10 μM) for 24 h. Cell death was detected by Hoechst 33342 /PI staining and data were analysed (white arrows: apoptotic vesicles), scale bar = 10 μm. (**C** and **D**) Apoptosis of melanoma cells was detected by TUNEL staining and the apoptosis rate was analysed, scale bar = 50 μm. (**E** and **F**) Western blot was performed to detect and quantify the expression of apoptosis-related proteins in A375 and A2058 cells treated with different concentrations of SPP86 (0, 1, 5, 10 μM) for 24 h. α-Tubulin was used as an internal control. The data represent the mean ± SD from five independent experiments. ***P < 0.001.
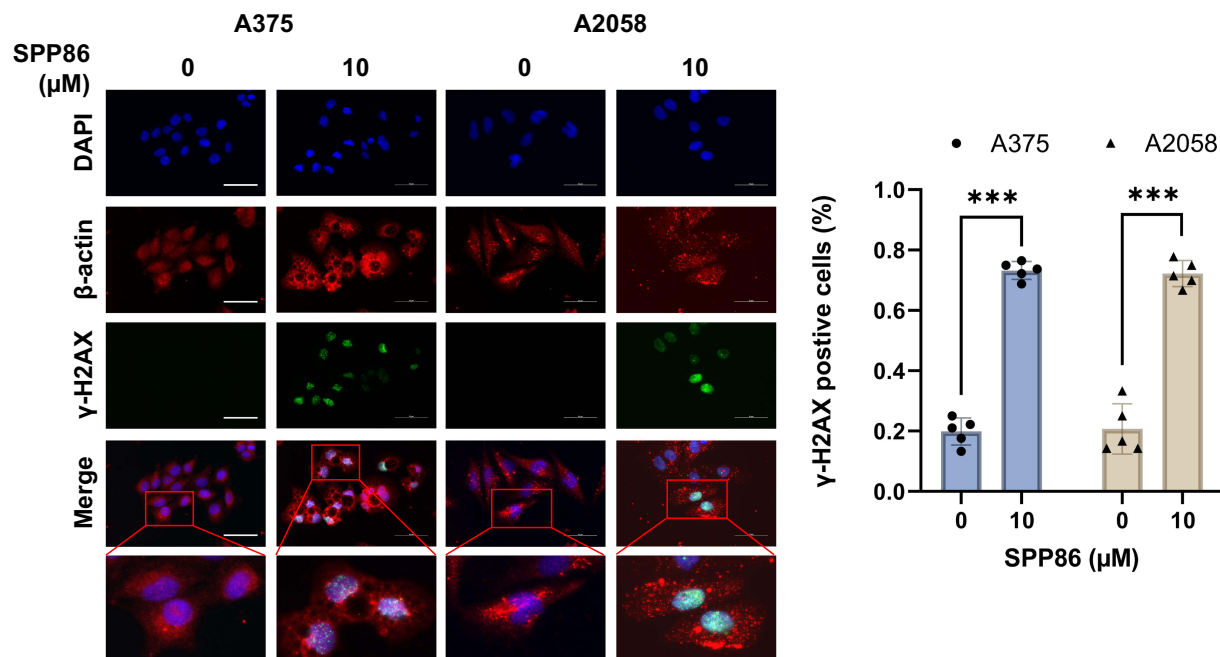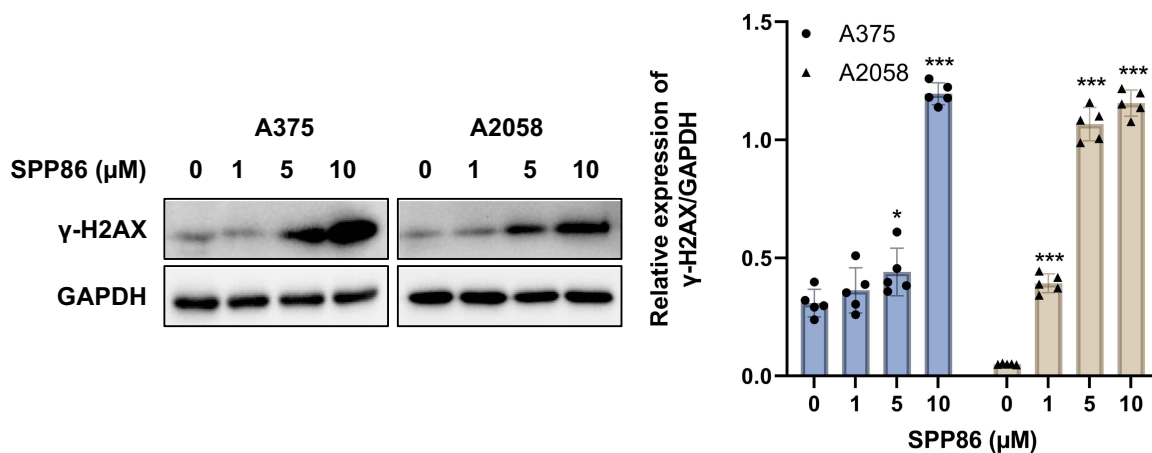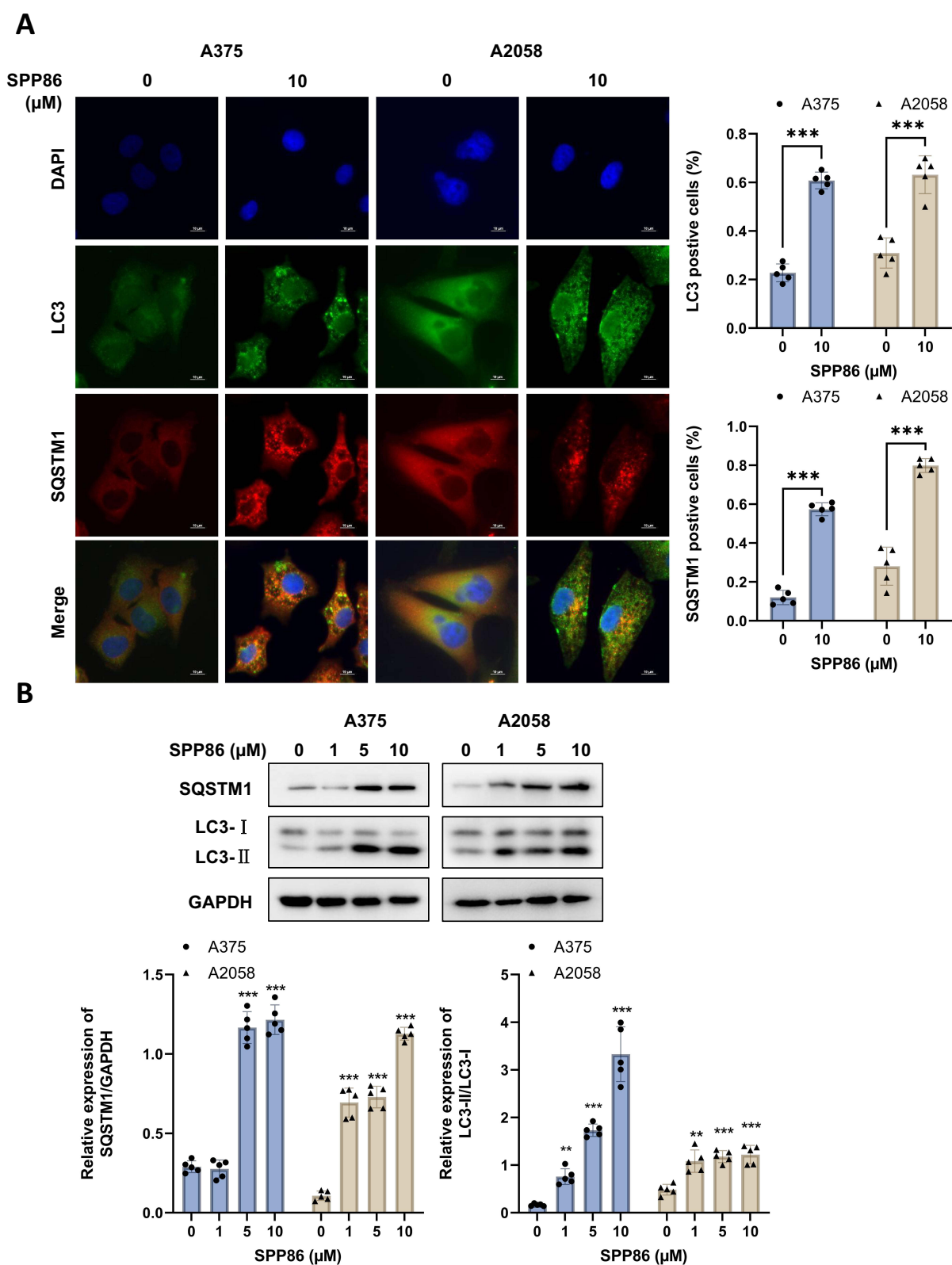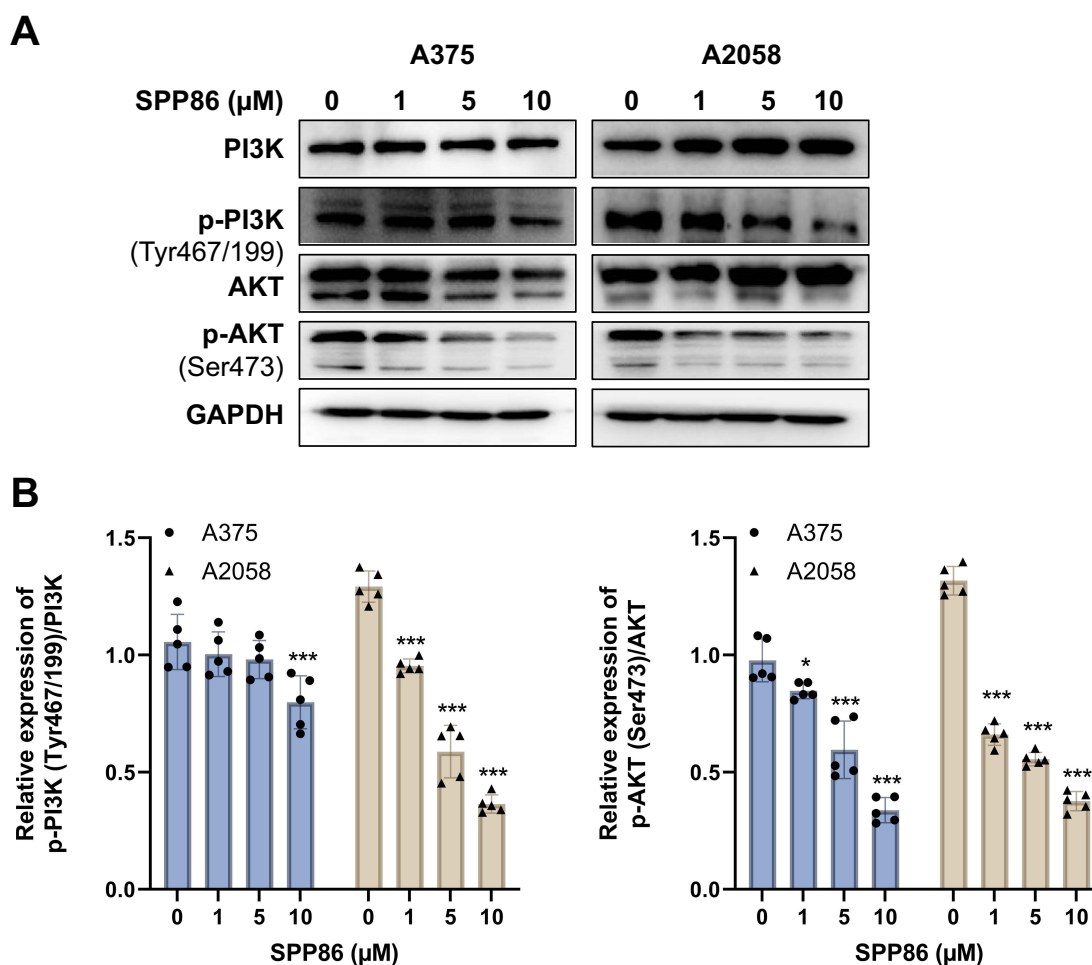
Figure 4 SPP86 induces DNA damage in melanoma cells. (**A**) Localisation of γ-H2AX expression in A375 and A2058 cells was detected by Immunofluorescence after treatment with SPP86 (10 μM) for 24 h, Scale bar = 50 μm. (**B**) Western blot was performed to detect and quantify the expression of γ-H2AX in A375 and A2058 cells treated with different concentrations of SPP86 (0, 1, 5, 10 μM) for 24 h. GAPDH was used as an internal control. The data represent the mean ± SD from five independent experiments. *$P < 0.05$, ***$P < 0.001$.

SPP86 Inhibits the PI3K/AKT Signaling Pathway

The PI3K/AKT signaling pathway plays a crucial role in regulating cell growth, development, and progression. To investigate the effect of SPP86 on the PI3K/AKT pathway, cells were treated with SPP86 for 24 h. Western blot analysis was performed to assess the phosphorylation and overall levels of PI3K and AKT in A375 and A2058 cells. The levels of p-PI3K and p-AKT were significantly reduced after SPP86 treatment in a dose-dependent manner. This suggests that SPP86 inhibits the PI3K/AKT pathway in melanoma cells (Figure 6A and B).

Figure 5 SPP86 inhibits autophagy in melanoma cells. (**A**) A375 and A2058 cells were treated with SPP86 (10 μM) for 24 h. Changes in the expression of key indicators of autophagy (LC3, SQSTM1) were detected and analysed by Immunoluminescence, Scale bar = 10 μm. (**B**) Expression of SQSTM1 and LC3-I, LC3-II in A375 and A2058 cells after 24 h of action of different concentrations of SPP86 (0, 1, 5, 10 μM) and data were analysed. GAPDH was used as an internal control. The data represent the mean ± SD from five independent experiments. **$*P < 0.01$, ***$P < 0.001$.

Figure 6 SPP86 inhibited PI3K/AKT signaling pathway in melanoma cells. (**A**) Cells were treated with SPP86 (0, 1, 5.10 μM) for 24 h, the protein expression levels of PI3K, p-PI3K (Tyr467/199), AKT, p-AKT (Ser473) in A375 and A2058 cells were determined by Western blot. GAPDH was used as an internal control. (**B**) Quantitative analysis of the protein expression levels of p-PI3K(Tyr467/199)/PI3K, p-AKT (Ser473)/AKT in A375 and A2058 cells. The data represent the mean ± SD from five independent experiments. *$P < 0.05$, ***$P < 0.001$.

The Activation of the PI3K/AKT Signaling Pathway Counteracts Partial of the Effects of SPP86 on Melanoma Cell Proliferation, Apoptosis, and DNA Damage

To further verify the role of SPP86 in the PI3K/AKT signaling pathway, we added the PI3K agonist YS-49 and subsequently treated the cells with SPP86. We assessed the proliferation, apoptosis and DNA damage of melanoma cells after treatment with YS-49 and SPP86 using CCK-8, Western blot, Flow cytometry, and Immunofluorescence.

First, we measured the proliferation rates of A375 and A2058 cells. As shown in Figure S3A, co-treatment with YS-49 and SPP86 significantly increased the proliferation rates of A375 and A2058 cells compared to the SPP86-only group. Next, we analyzed the expression of AKT, a key protein in the PI3K/AKT pathway, via Western blot. As illustrated in Figure S3B, co-treatment with YS-49 and SPP86 significantly upregulated the expression of phosphorylated AKT (ser473) compared to the SPP86-only group.

We then assessed the apoptosis rates of A375 and A2058 cells using Flow cytometry. As shown in Figure S3C, the co-treatment group of YS-49 and SPP86 exhibited a significantly reduced apoptosis rate in A375 and A2058 cells compared to the SPP86 treatment group. Additionally, we measured the expression of the apoptotic marker PARP1 using Western blot. As demonstrated in Figure S3B, PARP1 protein expression was significantly decreased in the YS-49 and SPP86 co-treatment group compared to the SPP86-only group.

Finally, we evaluated the expression of γ-H2AX in A375 and A2058 cells through Immunofluorescence. As shown in Figure S3D, the expression of γ-H2AX was significantly reduced in the YS-49 co-treated group compared to the SPP86-

only group. This finding was further confirmed by Western blot, which revealed a significant decrease in γ-H2AX protein levels in the YS-49 and SPP86 co-treatment group compared to the SPP86 group, as shown in Figure S3B.

These results indicate that YS-49 activates the PI3K/AKT signaling pathway, counteracting some of the effects of SPP86 on melanoma cell proliferation inhibition, apoptosis promotion, and DNA damage induction. This suggests that SPP86 may directly influence the PI3K/AKT signaling pathway, thereby exerting its effects on the inhibition of melanoma cell proliferation, promotion of apoptosis, and induction of DNA damage.

Modulating Autophagy Interferes with the Antiproliferative and Pro-Apoptotic Effects of SPP86 on Melanoma Cells

To confirm the role of autophagy in tumor suppression by SPP86, A375 cells were treated with SPP86 in combination with Rapamycin (an autophagy activator), or Baf A1 (an autophagy inhibitor).

The expression levels of LC3-II/I and SQSTM1 were assessed by Western blot analysis 24 h post co-treatment. The results showed that the combination of Baf A1 and SPP86 significantly reduced the protein level of LC3B-II/I and increased the expression of SQSTM1 in A375 cells compared with the SPP86 group alone. This suggests that the combination of SPP86 and Baf A1 further inhibited the autophagy in the cells. On the other hand, the combination of Rapamycin and SPP86 significantly increased the protein level of LC3B-II/I and decreased the expression of SQSTM1 in A375 cells compared with that of SPP86 alone. This suggests that the combination of SPP86 and Rapamycin enhanced autophagy in the cells (Figure 7A).

Subsequently, a CCK-8 assay was performed to assess changes in cell viability. Cell viability was significantly decreased in the SPP86 combined with Baf A1 group compared to the SPP86 alone group, suggesting that further inhibition of autophagy could enhance the ability of SPP86 to inhibit cell proliferation. On the contrary, in the SPP86 co-administered with Rapamycin group, A375 cell viability was increased, suggesting that activating autophagy in the cells weakened the ability of SPP86 to inhibit cell proliferation (Figure 7B).

Apoptosis was detected using a TUNEL assay, and SPP86 in combination with Baf A1 or Rapamycin significantly increased or decreased the apoptosis rate of A375 cells, respectively, compared with the SPP86 alone group (Figure 7C and D). Then we examined the effect of SPP86 on apoptosis of melanoma cells by Flow cytometry using Annexin V-FITC/PI Apoptosis Detection Kit. Compared to the SPP86 treatment alone, the combination of SPP86 with Baf A1 significantly increased the apoptosis rate of A375 cells, while the combination with Rapamycin led to a significant decrease in apoptosis (Figure S4).

In addition, Western blot was performed to evaluate the expression level of cleaved PARP1, and the results were consistent with the TUNEL assay (Figure 7E). Taken together, this suggests that inhibition of autophagy enhances the antiproliferative and pro-apoptotic effects of SPP86 on melanoma cells.

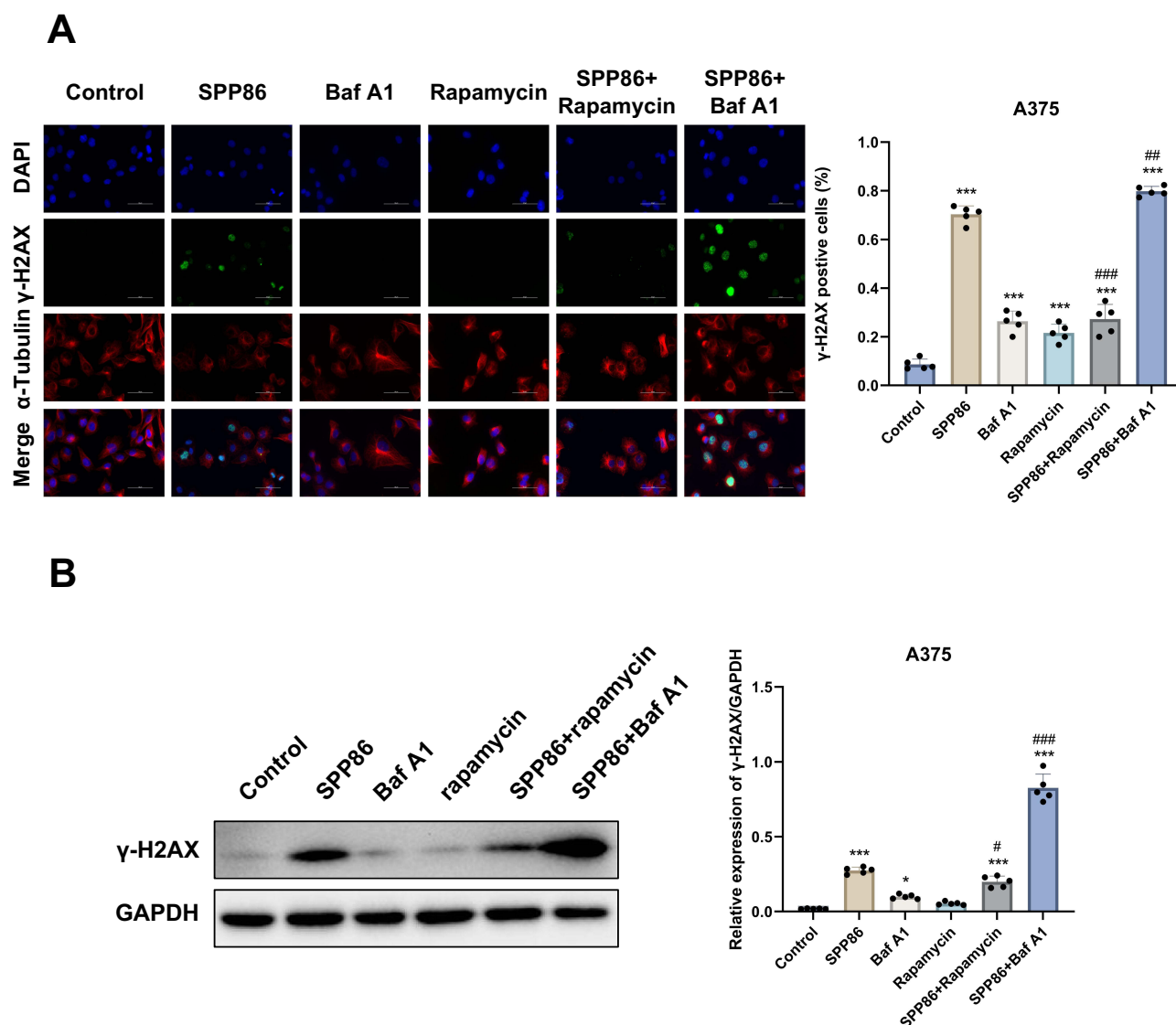## Inhibition of Autophagy Accelerates SPP86-Induced γ-H2AX Formation

To further investigate the potential impact of autophagy regulation on SPP86-induced DNA damage in melanoma cells, the changes in γ-H2AX fluorescence were detected following modulation of autophagy. It was observed that the intensity of γ-H2AX fluorescence was significantly enhanced in the SPP86 combined with Baf A1 group compared with the SPP86 alone group (Figure 8A). Meanwhile, Western blot also confirmed the significant upregulation of γ-H2AX expression in the SPP86 combined with Baf A1 group (Figure 8B). This suggests that inhibition of autophagy enhances SPP86-induced γ-H2AX lesion formation. This further supports the notion that inhibition of autophagy enhances SPP86-induced DNA damage response.

Discussion

The results of this study reveal that SPP86 effectively inhibits melanoma cell proliferation, induces apoptosis, and promotes DNA damage, while also suppressing the PI3K/AKT signaling pathway. Additionally, SPP86 disrupts cellular autophagy, which may influence its anti-proliferative, pro-apoptotic, and DNA damage in melanoma cells. The identification of SPP86 as
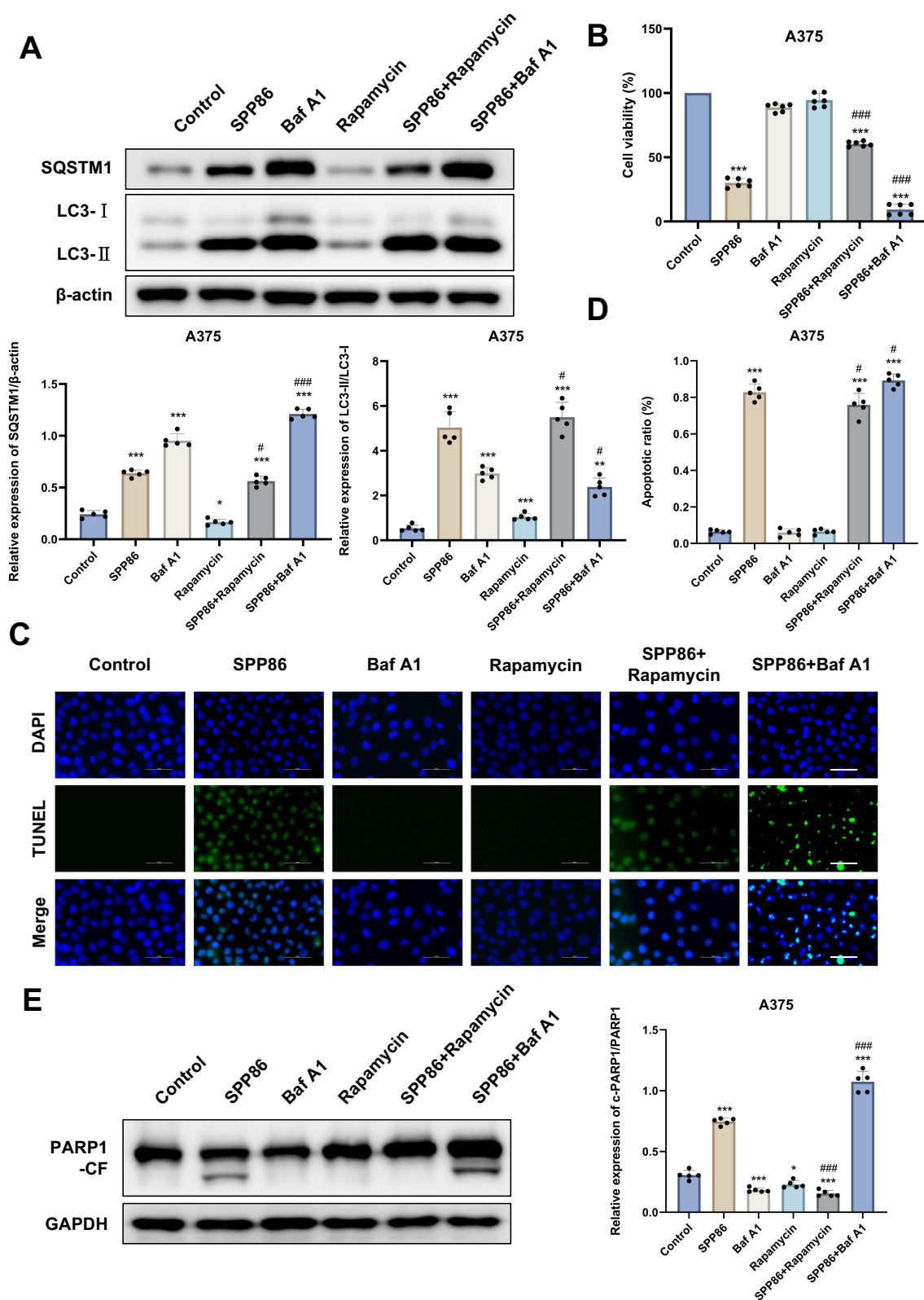
Figure 7 Modulation of autophagy interferes with the proliferation inhibition and pro-apoptotic effects of SPP86 on melanoma cells. (**A**) Combining SPP86 (10 μM) with Baf A1 (100 nmol/L) or Rapamycin (10 nmol/L) for 24 h resulted in decreased or increased levels of autophagy in A375 cells compared with SPP86 alone, respectively, as determined by Western blot. β-actin was used as an internal control. (**B**) CCK-8 assay showed an lower cell viability in the presence of SPP86 and Baf A1, the cell viability was increased with the combination of SPP86 and Rapamycin, compared with SPP86 alone. (**C** and **D**) TUNEL analysis showed the concurrent application of SPP86 with Baf A1 or Rapamycin resulted in a notable augmentation or reduction, respectively in the rate of apoptosis compared with SPP86 alone, Scale bar = 50 μm. (**E**) Western blot was performed to detect changes in the expression of the apoptotic protein PARP1 and data were analysed. GAPDH was used as internal loading reference. The data represent the mean ± SD from five independent experiments. *$P < 0.01$, **$P < 0.01$, ***$P < 0.001$: drug-dosing group VS Control. #$P < 0.05$, ###$P < 0.001$: co-dosing group VS SPP86.

A

B

Figure 8 Inhibition of autophagy accelerates SPP86-induced γ-H2AX formation. (**A**) Immunofluorescence analysis of the expression level of γ-H2AX, an indicator of DNA damage in A375 cells, was increased or decreased by SPP86 (10 μM) in combination with Baf A1 (100 nM) or Rapamycin (10 nM), respectively, compared with that of SPP86 alone, after 24 h. The expression level of γ-H2AX, an indicator of DNA damage, was increased or decreased by Immunofluorescence analysis, respectively, compared with that of SPP86 alone, Scale bar = 50 μm. (**B**) Western blot was performed to detect changes in the expression of the apoptotic protein γ-H2AX and data were analysed. GAPDH was used as internal loading reference. The data represent the mean ± SD from five independent experiments. *$P < 0.05$, ***$P < 0.001$: drug-dosing group VS Control. #$P < 0.05$, ###$P < 0.001$: co-dosing group VS SPP86.

a targeted small molecule inhibitor holds significant promise for melanoma therapy and opens new avenues for further investigation in this domain.

The persistent underperformance of therapies for advanced melanoma has intensified the exploration of new anti-melanoma compounds.[19] SPP86, a targeted small molecule inhibitor, has been shown to effectively target RET tyrosine kinase and suppress critical signaling pathways such as PI3K/AKT and MAPK, which are instrumental in cell migration and differentiation.[13,20,21] In a preclinical evaluation of novel tyrosine kinase inhibitors in medullary thyroid carcinoma, SPP86 was identified as the most potent inhibitor of tumor cell proliferation.[9] Despite this, the efficacy of SPP86 in treating melanoma has not been extensively studied. Our investigation demonstrates that SPP86 significantly reduces melanoma cell proliferation and viability and impairs the colony-forming ability of these cells in a dose-dependent manner. These results suggest that SPP86 has considerable potential as a therapeutic option for managing melanoma.

Given that PARP1 activation predominantly occurs in response to DNA damage, our findings suggest an association between SPP86 treatment and DNA damage in melanoma cells. The DNA damage response (DDR) is critical for maintaining genomic stability,[22] and numerous compounds targeting DDR pathways have been rigorously examined in clinical trials, demonstrating promising results in cancer management.[23–26] Analogous to certain anticancer drugs like cisplatin, which are known to induce DNA damage and consequently trigger apoptosis,[27–30] SPP86 in our study was demonstrated to cause phosphorylation of H2AX, a hallmark of cellular DNA damage, thereby initiating apoptosis.

Phosphoinositide 3-kinases (PI3Ks) play a pivotal role in a myriad of cellular signaling pathways, with a particularly notable impact on cancer progression.[31] The PI3K/AKT signaling pathway, often activated by growth factors and hormone receptors, is crucial for promoting cell proliferation, survival, and motility, while also inhibiting apoptosis.[32] AKT, which is directly activated by PI3K, initiates a cascade of signals that significantly contribute to tumorigenesis.[33] Our study indicates that the inhibitory effects of SPP86 on melanoma cells might be attributed to its ability to block the activation of phosphorylated PI3K (p-PI3K) and phosphorylated AKT (p-AKT), key players in the melanoma cell survival and growth.

The intricate relationship between autophagy and cancer progression has been increasingly recognized, with autophagy serving as a crucial component in a spectrum of physiological and pathological states.[34–37] To elucidate the role of autophagy in the anticancer effects of SPP86, our study employed Immunofluorescence analysis and Western blot techniques. We observed that SPP86 treatment significantly increased the LC3-II/I ratio and also led to the accumulation of SQSTM1 protein levels. The conversion of LC3-I to the lipidated form LC3-II is a vital step in autophagosome formation, whereas the buildup of SQSTM1 suggests an impairment in the autophagic flux, indicating a bottleneck in the maturation of autophagosomes into autolysosomes. Consequently, the data imply that SPP86 exerts an inhibitory influence on autophagy within the cellular context.

Once a tumor is established, autophagy becomes the primary survival mechanism of tumor cells, supplying nutrients for their growth, aiding in their evasion of the cytotoxic effects of radiotherapy or chemotherapy, and shielding them from apoptosis.[38] Chunrong discovered that the expression levels of autophagy-related genes were positively associated with metastasis and poor prognoses in melanoma.[39] In the current study, we sought to ascertain the autophagy-related tumor-suppressive functions of SPP86. We observed that SPP86's ability to inhibit cell proliferation and promote apoptosis, as well as to induce DNA damage in melanoma cells, was modulated by the autophagic pathway. The inhibition of autophagy with Bafilomycin A1 augmented the antiproliferative effect of SPP86 on melanoma cells. When used in combination, SPP86 and Bafilomycin A1 induced a greater degree of apoptosis and DNA damage in A375 melanoma cells. In contrast, these effects were mitigated upon the induction of autophagy with rapamycin. These findings are in line with previous work suggesting that the concomitant inhibition of ERK and autophagy may be beneficial in KRAS-mutant pancreatic cancer,[40,41] thereby supporting the potential of integrating targeted therapy with autophagy inhibition in cancer treatment.[42] Moreover, our results indicate that the autophagy-inhibiting action of SPP86 plays a significant role in enhancing DNA damage and apoptosis, bolstering the candidacy of SPP86 as a promising therapeutic agent for melanoma.

In conclusion, the present study confirmed that SPP86 induces apoptosis and activates the DNA damage response by inhibiting autophagy and the PI3K/AKT signaling pathway in melanoma cells. Although the use of immortalized cell lines with BRAFWT mutations has some limitations, and the tumor growth inhibitory effect of SPP86 in vivo needs to be further investigated. Nevertheless, these findings provide a strong foundation for future research into the potential anti-melanoma activity of targeting RET.

Conclusion

The study demonstrated that SPP86 exerts anti-tumor effects in melanoma cells through multiple mechanisms: it induces apoptosis, causes DNA damage, inhibits cell proliferation, and suppresses the PI3K/AKT signaling pathway. Importantly, the inhibition of autophagy appears to be a critical component of SPP86's mode of action, with the modulation of autophagic processes influencing the cytotoxicity against melanoma cells. These insights contribute to our understanding of the complex biological underpinnings that could be leveraged in developing innovative and multifaceted therapeutic approaches for melanoma. Given these promising findings, SPP86 emerges as a potential therapeutic candidate for the treatment of cutaneous melanoma, warranting further investigation and development.

Abbreviations

MM, Malignant melanoma; CM, Cutaneous melanoma; RTK, receptor tyrosine kinases; RET, Rearranged during Transfection; Baf A1, bafilomycin A1; PI3Ks, Phosphoinositide 3-kinases.

Funding

Disclosure

The authors declare that there are no conflicts of interest in this work.

References

1. Naik PP. Cutaneous Malignant Melanoma: a Review of Early Diagnosis and Management. *World Journal of Oncology*. 2021;12(1):7–19. doi:10.14740/wjon1349
2. Hartman RI, Lin JY. Cutaneous Melanoma-A Review in Detection, Staging, and Management. *Hematol Oncol Clin n*. 2019;33:25–38. doi:10.1016/j.hoc.2018.09.005
3. Iglesias-Pena N, Paradela S, Tejera-Vaquerizo A, Boada A, Fonseca E. Cutaneous Melanoma in the Elderly: review of a Growing Problem. *Actas Dermosifiliogr*. 2019;110:434–447. doi:10.1016/j.ad.2018.11.009
4. Orzan OA, Șandru A, Jecan CR. Controversies in the diagnosis and treatment of early cutaneous melanoma. *J Med Life*. 2015;8:132–141.
5. Țăpoi DA, Derewicz D, Gheorghișan-Gălățeanu AA, Dumitru AV, Ciongariu AM, Costache M. The Impact of Clinical and Histopathological Factors on Disease Progression and Survival in Thick Cutaneous Melanomas. *Biomedicines*. 2023;11:null. doi:10.3390/biomedicines11102616
6. Leonardi GC, Falzone L, Salemi R, et al. Cutaneous melanoma: from pathogenesis to therapy (Review). *Int j Oncol*. 2018;52:1071–1080. doi:10.3892/ijo.2018.4287
7. Lugović-Mihić L, Ćesić D, Vuković P, Novak Bilić G, Šitum M, Špoljar S. Melanoma Development. Current Knowledge on Melanoma Pathogenesis. *Acta dermatovener cr*. 2019;27:163–168.
8. Shen Q, Han Y, Wu K, et al. MrgprF acts as a tumor suppressor in cutaneous melanoma by restraining PI3K/AKT signaling. *Signal Transduction Tar*. 2022;7:147. doi:10.1038/s41392-022-00945-9
9. Saronni D, Gaudenzi G, Dicitore A, et al. Preclinical Evaluation of Novel Tyrosine-Kinase Inhibitors in Medullary Thyroid Cancer. *Cancers*. 2022;14:null. doi:10.3390/cancers14184442
10. Ottaviano M, F GE, Tortora M, et al. BRAF gene and melanoma: back to the future. *Int J Mol Sci*. 2021;22(7):3474. doi:10.3390/ijms22073474
11. Peyssonnaux C, Eychene A. The Raf/MEK/ERK pathway: new concepts of activation. *Biol Cell*. 2001;93:53–62. doi:10.1016/s0248-4900(01)01125-x
12. Silva JM, Bulman C, McMahon M. BRAFV600E cooperates with PI3K signaling, independent of AKT, to regulate melanoma cell proliferation. *Mol Cancer Res*. 2014;12:447–463. doi:10.1158/1541-7786.MCR-13-0224-T
13. Alao JP, Michlikova S, Dinér P, Grøtli M, Sunnerhagen P. Selective inhibition of RET mediated cell proliferation in vitro by the kinase inhibitor SPP86. *BMC Cancer*. 2014;14:853. doi:10.1186/1471-2407-14-853
14. Xu Z, Han X, Ou D, et al. Targeting PI3K/AKT/ mTOR-mediated autophagy for tumor therapy. *Appl microbiol biot*. 2020;104:575–587. doi:10.1007/s00253-019-10257-8
15. Yousefi S, Simon HU. Autophagy in cancer and chemotherapy. *Results Probl Cell Differ*. 2009;49:183–190. doi:10.1007/400_2008_25
16. Rahmati M, Ebrahim S, Hashemi S, Motamedi M, Moosavi MA. New insights on the role of autophagy in the pathogenesis and treatment of melanoma. *Mol biol rep*. 2020;47:9021–9032. doi:10.1007/s11033-020-05886-6
17. Hu S. Inhibition of Autophagy by Berbamine Hydrochloride Mitigates Tumor Immune Escape by Elevating MHC-I in Melanoma Cells. *Cells*. 2024;13(18). doi:10.3390/cells13181537
18. Mehnert JM, Mitchell TC, Huang AC, et al. BAMM (BRAF autophagy and MEK inhibition in melanoma): a phase I/II trial of Dabrafenib, trametinib, and hydroxychloro- quine in advanced BRAFV600-mutant melanoma. *Clin Cancer Res*. 2022;28(6):1098–1106. doi:10.1158/1078-0432.CCR-21-3382
19. Li JK, Zhu PL, Wang Y, et al. Gracillin exerts anti-melanoma effects in vitro and in vivo: role of DNA damage, apoptosis and autophagy. *Phytomedicine*. 2023;108:154526. doi:10.1016/j.phymed.2022.154526
20. Castellano E, Molina-Arcas M, Krygowska AA, et al. RAS signalling through PI3-Kinase controls cell migration via modulation of Reelin expression. *Nat Commun*. 2016;7:11245. doi:10.1038/ncomms11245
21. Crupi MJF, Maritan SM, Reyes-Alvarez E, et al. GGA3-mediated recycling of the RET receptor tyrosine kinase contributes to cell migration and invasion. *Oncogene*. 2020;39:1361–1377. doi:10.1038/s41388-019-1068-z
22. Brandsma I, Fleuren EDG, Williamson CT, Lord CJ. Directing the use of DDR kinase inhibitors in cancer treatment. *Expert Opin Inv Drug*. 2017;26:1341–1355. doi:10.1080/13543784.2017.1389895
23. Fok JHL, Ramos-Montoya A, Vazquez-Chantada M, et al. AZD7648 is a potent and selective DNA-PK inhibitor that enhances radiation, chemotherapy and olaparib activity. *Nat Commun*. 2019;10:5065. doi:10.1038/s41467-019-12836-9
24. Ricciuti B, Recondo G, Spurr LF, et al. Impact of DNA Damage Response and Repair (DDR) Gene Mutations on Efficacy of PD-(L)1 Immune Checkpoint Inhibition in Non-Small Cell Lung Cancer. *Clin Cancer Res*. 2020;26:4135–4142. doi:10.1158/1078-0432.CCR-19-3529
25. Sheng H, Huang Y, Xiao Y, et al. ATR inhibitor AZD6738 enhances the antitumor activity of radiotherapy and immune checkpoint inhibitors by potentiating the tumor immune microenvironment in hepatocellular carcinoma. *J Immunother Cancer*. 2020;8. doi:10.1136/jitc-2019-000340

https://doi.org/10.2147/DDDT.S473390

26. Wengner AM, Siemeister G, Lücking U, et al. The Novel ATR Inhibitor BAY 1895344 Is Efficacious as Monotherapy and Combined with DNA Damage-Inducing or Repair-Compromising Therapies in Preclinical Cancer Models. *Mol Cancer Ther.* 2020;19:26–38. doi:10.1158/1535-7163. MCT-19-0019

27. Ghosal G, Chen J. DNA damage tolerance. a double-edged sword guarding the genome. *Transl Cancer Res.* 2013;2:107–129. doi:10.3978/j. issn.2218-676X20130401

28. Jackson JR, Gilmartin A, Imburgia C, Winkler JD, Marshall LA, Roshak A. An indolocarbazole inhibitor of human checkpoint kinase (Chk1) abrogates cell cycle arrest caused by DNA damage. *Cancer Res.* 2000;60:566–572.

29. van Jaarsveld MTM, Deng D, Ordoñez-Rueda D, Paulsen M, Wiemer EAC, Zi Z. Cell-type-specific role of CHK2 in mediating DNA damage-induced G2 cell cycle arrest. *Oncogenesis.* 2020;9:35. doi:10.1038/s41389-020-0219-y

30. Allday MJ, Inman GJ, Crawford DH, Farrell PJ. DNA damage in human B cells can induce apoptosis, proceeding from G1/S when p53 is transactivation competent and G2/M when it is transactivation defective. *EMBO j.* 1995;14:4994–5005. doi:10.1002/j1460-2075.1995.tb00182.x

31. Bradley D. Biography of Lewis C. Cantley. *Proc Natl Acad Sci U S A.* 2004;101:3327–3328. doi:10.1073/pnas.0400872101

32. Chang F, Lee JT, Navolanic PM, et al. Involvement of PI3K/AKT pathway in cell cycle progression, apoptosis, and neoplastic transformation: a target for cancer chemotherapy. *Leukemia.* 2003;17:590–603. doi:10.1038/sj.leu.2402824

33. Cheng L, Wang H, Wang Z, Huang H, Zhuo D, Lin J. Leflunomide Inhibits Proliferation and Induces Apoptosis via Suppressing Autophagy and PI3K/AKT Signaling Pathway in Human Bladder Cancer Cells. *Drug Des Devel Ther.* 2020;14:1897–1908. doi:10.2147/DDDT.S252626

34. Yu L, Strandberg L, Lenardo MJ. The selectivity of autophagy and its role in cell death and survival. *Autophagy.* 2008;4:567–573. doi:10.4161/ auto.5902

35. Mizumura K, Choi AM, Ryter SW. Emerging role of selective autophagy in human diseases. *Front Pharmacol.* 2014;5:244. doi:10.3389/ fphar.2014.00244

36. Rubinsztein DC, Codogno P, Levine B. Autophagy modulation as a potential therapeutic target for diverse diseases. *Nat Rev Drug Discov.* 2012;11:709–730. doi:10.1038/nrd3802

37. Amaravadi RK, Lippincott-Schwartz J, Yin XM, et al. Principles and current strategies for targeting autophagy for cancer treatment. *Clin Cancer Res.* 2011;17:654–666. doi:10.1158/1078-0432.CCR-10-2634

38. Kimmelman AC. The dynamic nature of autophagy in cancer. *Gene dev.* 2011;25:1999–2010. doi:10.1101/gad.17558811

39. Han C, Sun B, Wang W, et al. Overexpression of microtubule-associated protein-1 light chain 3 is associated with melanoma metastasis and vasculogenic mimicry. *Tohoku j exp med.* 2011;223:243–251. doi:10.1620/tjem.223.243

40. Bryant KL, Stalnecker CA, Zeitouni D, et al. Combination of ERK and autophagy inhibition as a treatment approach for pancreatic cancer. *Nat med.* 2019;25:628–640. doi:10.1038/s41591-019-0368-8

41. Kinsey CG, Camolotto SA, Boespflug AM, et al. Protective autophagy elicited by RAF→MEK→ERK inhibition suggests a treatment strategy for RAS-driven cancers. *Nat med.* 2019;25:620–627. doi:10.1038/s41591-019-0367-9

42. Wang H, Liang Y, Zhang T, et al. C-IGF1R encoded by cIGF1R acts as a molecular switch to restrict mitophagy of drug-tolerant persister tumour cells in non-small cell lung cancer. *Cell Death Differ.* 2023;30:2365–2381. doi:10.1038/s41418-023-01222-0